

# Tubulin Binding Sites on $\gamma$ -Tubulin: Identification and Molecular Characterization<sup>†</sup>

Roxana Llanos,<sup>‡</sup> Véronique Chevrier,<sup>‡</sup> Michel Ronjat,<sup>§</sup> Patricia Meurer-Grob,<sup>||</sup> Pascal Martinez,<sup>⊥</sup> Ronald Frank,<sup>▽</sup> Michel Bornens,<sup>○</sup> Richard H. Wade,<sup>||</sup> Juergen Wehland,<sup>∞</sup> and Didier Job<sup>\*,‡</sup>

Département de Biologie Moléculaire et Structurale, CEA de Grenoble, 17 Rue des Martyrs, 38054 Grenoble Cedex 9, France, LMES, IBS, 41 Rue Jules Horowitz, 38027 Grenoble Cedex 1, France, AG Molecular Recognition and Division of Cell Biology and Immunology, Gesellschaft für Biotechnologische Forschung, Mascheroder Weg 1, D-38124 Braunschweig, Germany, and UMR 144 du Centre National de la Recherche Scientifique, Section de Recherche, Institut Curie, 26 Rue d'Ulm, 75231 Paris Cedex 05, France

Received April 19, 1999; Revised Manuscript Received August 24, 1999

**ABSTRACT:**  $\gamma$ -Tubulin is essential to microtubule organization in eukaryotic cells. It is believed that  $\gamma$ -tubulin interacts with tubulin to accomplish its cellular functions. However, such an interaction has been difficult to demonstrate and to characterize at the molecular level.  $\gamma$ -Tubulin is a poorly soluble protein, not amenable to biochemical studies in a purified form as yet. Therefore basic questions concerning the existence and properties of tubulin binding sites on  $\gamma$ -tubulin have been difficult to address. Here we have performed a systematic search for tubulin binding sites on  $\gamma$ -tubulin using the SPOT peptide technique. We find a specific interaction of tubulin with six distinct domains on  $\gamma$ -tubulin. These domains are clustered in the central part of the  $\gamma$ -tubulin primary amino acid sequence. Synthetic peptides corresponding to the tubulin binding domains of  $\gamma$ -tubulin bind with nanomolar  $K_d$ s to tubulin dimers. These peptides do not interfere measurably with microtubule assembly in vitro and associate with microtubules along the polymer length. On the tertiary structure, the  $\gamma$ -tubulin peptides cluster to surface regions on both sides of the molecule. Using SPOT analysis, we also find peptides interacting with  $\gamma$ -tubulin in both the  $\alpha$ - and  $\beta$ -tubulin subunits. The tubulin peptides cluster to surface regions on both sides of the  $\alpha$ - and  $\beta$ - subunits. These data establish  $\gamma$ -tubulin as a tubulin ligand with unique tubulin-binding properties and suggests that  $\gamma$ -tubulin and tubulin dimers associate through lateral interactions.

In most animal cells, the correct assembly and organization of microtubules is controlled by the centrosome. This structure contains a poorly defined pericentriolar material that surrounds a pair of cylinders of nine microtubule triplets called the centrioles. Cytoplasmic microtubules nucleate from the pericentriolar material (for reviews see refs 1 and 2). The slow-growing (minus) end of a microtubule is attached to the pericentriolar material, whereas the rapidly growing (plus) end extends away from the centrosome. There is evidence that microtubule nucleation on centrosomes depends on the association of the pericentriolar material with protein complexes that contain  $\gamma$ -tubulin (3–10). This protein is part of the tubulin superfamily. The  $\gamma$ -tubulin gene, *mipA*, from the filamentous fungus *Aspergillus nidulans* was first identi-

fied as a suppressor of a conditional and lethal mutation in  $\beta$ -tubulin (11). The amino acid sequence of this protein and its subcellular localization to MTOCs is evolutionarily conserved in animals, plants and fungi (for reviews see 12 and 13). Genetic, structural, and biochemical analyses implicate  $\gamma$ -tubulin as having an essential role in microtubule organization (9, 13). In *A. nidulans*,  $\gamma$ -tubulin is not absolutely required for microtubule nucleation (14) and its role in microtubule organization probably extends beyond its apparent function in microtubule nucleation. In mammalian cells, current models of centrosome-directed microtubule nucleation involve a direct interaction of  $\gamma$ -tubulin with tubulin  $\alpha/\beta$  dimers. So far, however, evidence for direct interaction between  $\gamma$ -tubulin and tubulin has been lacking. To study the biochemistry of the process has been difficult, since  $\gamma$ -tubulin is a minor protein in the cell that cannot be overproduced in a soluble form by genetic engineering (15–17). In vitro translated  $\gamma$ -tubulin cosediments with microtubules in microtubule binding assays but one cannot exclude that it forms complexes with other proteins in the cell extract used for in vitro translation. Melki et al. (18) have demonstrated that extensively purified (but not homogeneous)  $\gamma$ -tubulin binds to microtubules following renaturation in the presence of a chaperonin. However, only minute amounts of renatured  $\gamma$ -tubulin were obtained and this did not favor detailed biochemical analysis. To study the interaction of  $\gamma$ -tubulin with tubulin in vivo has also been difficult.  $\gamma$ -Tubulin is present in the cell cytoplasm but does not form

<sup>†</sup> This work was supported by grants from ARC and La Ligue to D.J. R.L. was supported by a postdoctoral fellowship from INSERM during this work.

\* To whom correspondence should be addressed: Tel 33 04 76 88 38 01; Fax 33 04 76 88 50 57, E-mail job@dsvgre.cea.fr.

<sup>‡</sup> INSERM U366, DBMS/CS, CEA de Grenoble.

<sup>§</sup> DBMS/CIS, CEA de Grenoble.

<sup>||</sup> LMES, IBS.

<sup>⊥</sup> DBMS/BECP, CEA de Grenoble.

<sup>▽</sup> AG Molecular Recognition, Gesellschaft für Biotechnologische Forschung.

<sup>○</sup> Institut Curie.

<sup>∞</sup> Division of Cell Biology and Immunology, Gesellschaft für Biotechnologische Forschung.

<sup>1</sup> Abbreviations: tubulin,  $\alpha/\beta$ -tubulin; MTOCs, microtubules organizing centers;  $\gamma$ TuRC,  $\gamma$ -tubulin ring complex.

simple bimolecular complexes with tubulin. Instead it interacts with other cell components to form multimolecular complexes (3–10) that are inactive with regard to microtubule nucleation. This precludes the use of direct functional assays of the presumptive interaction between  $\gamma$ -tubulin and tubulin in cells.

In this work, we were interested in testing the existence and function of tubulin binding sites on  $\gamma$ -tubulin, using direct assays and excluding interference with other proteins. To do this we have performed a systematic mapping of tubulin binding domains in  $\gamma$ -tubulin using the SPOT peptide technique (19). We report the identification of high-affinity specific tubulin binding domains on  $\gamma$ -tubulin. On the tertiary structure, these peptides cluster to surface regions of  $\gamma$ -tubulin that may interact with corresponding lateral surfaces on both tubulin subunits.

## EXPERIMENTAL PROCEDURES

**Purification of Tubulin.** Tubulin was prepared from fresh bovine brain by two cycles of polymerization and depolymerization followed by chromatography on P11 phosphocellulose as described in Mitchison and Kirschner (20).

**In Vitro Translation of  $\gamma$ -Tubulin.** For in vitro translation of  $\gamma$ -tubulin we used human  $\gamma$ -tubulin cDNA cloned in pBluescript SK(+) (pH3), kindly provided by Dr. B. Oakley (21). Specific restriction sites were introduced by site-directed mutagenesis (Sculptor, Amersham, Les Ulis, France) for subcloning of  $\gamma$ -tubulin subdomains. A *Bgl*II/*Xba*I site was introduced directly upstream of the 5' end of the  $\gamma$ -tubulin cDNA. An *Xba*I/*Bam*HI site was created by replacing nucleotides 426–437 of the  $\gamma$ -tubulin cDNA nucleotide by TCTAGACGGATC. A *Bgl*II site was created by replacing nucleotides 1252–1266 of the  $\gamma$ -tubulin cDNA by ATGATCAGATCT. Finally, a *Bcl*II site was created at the 3' end of the  $\gamma$ -tubulin cDNA by replacing nucleotides 1372–1377 by ATGATC. From this construct, fragments of the  $\gamma$ -tubulin cDNA were subcloned in pBluescript KS(+) (Stratagene, La Jolla, CA) for in vitro translation of  $\gamma$ -tubulin subdomains.<sup>35</sup>S-Labeled full-length  $\gamma$ -tubulin and its domains were produced in vitro by using the TNT coupled transcription–translation system (Promega, Charbonnières, France) according to the manufacturer's instructions.

**SPOT Analysis.** SPOT synthesis was performed according to Frank (19) with an Abimed ASP 222 automated SPOT robot. This technique allows systematic epitope analysis of proteins whose amino acid sequence is known. Briefly, the amino acid sequence of the protein of interest was subdivided into overlapping peptides. In this study we used 15-mer peptides and the overlap was 12 amino acids. The overlapping peptides were synthesized spotwise on a cellulose membrane. Peptides were linked to the membrane through their C-terminal amino acid. Numbering amino acids from the C-terminal end of the protein, the first peptide contained amino acids 1–15, the second contained amino acids 4–19, and so on, to encompass the entire protein sequence. SPOT membranes were prepared for the following proteins: human  $\gamma$ -tubulin; porcine  $\alpha$ - and  $\beta$ -tubulins; bovine STOP protein (22), and human E-MAP115 (23). For overlay binding assays we used either <sup>32</sup>P-labeled bovine brain tubulin or <sup>35</sup>S-labeled  $\gamma$ -tubulin derivatives. Bovine brain tubulin (80 mg) was labeled with 40  $\mu$ Ci of [ $\alpha$ -<sup>32</sup>P]GTP (Amersham) by an

exchange reaction in PEM buffer (100 mM Pipes-KOH, pH 6.65, 1 mM EGTA, and 1 mM MgCl<sub>2</sub>) at 4 °C for 10 min and immediately used for binding assay. <sup>35</sup>S-Labeled full-length  $\gamma$ -tubulin and its domains were produced in vitro by using the TNT coupled transcription–translation system according to the manufacturer's instructions. Overlay binding assays were subsequently run according to Niebuhr and Wehland (24). Briefly, peptide sheets were washed three times (5 min each) with Tris-buffered saline (20 mM Tris-HCl and 140 mM NaCl, pH 7.6) with 0.1% Tween-20 (TBS-T) and saturated with blocking buffer (TBS-T plus 10% fetal calf serum) overnight at 4 °C. After being washed for 5 min with TBS-T, peptides sheets were incubated with radioactive labeled proteins. <sup>35</sup>S-Labeled proteins were incubated with SPOT sheets in blocking buffer (1 h at room temperature) and then washed for at least 5 min each with TBS-T, TBS-T plus 0.5 M NaCl, TBS-T plus 0.5% Triton X-100, and TBS-T and then exposed to a phosphorimager screen for 1 h. <sup>32</sup>P-Labeled tubulin was incubated with SPOT sheets in PEM containing 0.5% Triton X-100 (PEM-TX) and subsequent washes were done in PEM-TX-based buffers instead of TBS-T-based buffer. Relative binding values were determined by scanning the peptide sheets with a PhosphorImager with ImageQuant and MultiQuant softwares (Molecular Dynamics, Bondoufle, France) after 1 h of exposure.

**Peptide Synthesis.** Free, soluble peptides were synthesized with an Abimed ASP 222 multiple peptide synthesizer with TentaGel S resin (Rapp Polymere, Germany) and purified by HPLC. Free, soluble N-terminally biotinylated peptides were synthesized by Neosystems (Strasbourg, France) and purified by HPLC.

**$\gamma$ -Tubulin and Tubulin Antibodies.** For the development of peptide polyclonal antibodies, peptides were conjugated to keyhole limpet hemocyanin prior to injection into rabbits. Sera were affinity-purified against the corresponding peptide. Antibody  $\gamma$ 370 was developed against a peptide corresponding to amino acids 361–375 of  $\gamma$ -tubulin and reacted with the peptide sequence AHRVSG corresponding to amino acids 370–375 of  $\gamma$ -tubulin. Antibody  $\gamma$ 403 peptide was affinity-purified from a  $\gamma$ -tubulin polyclonal antiserum developed against bacterially expressed  $\gamma$ -tubulin, using immobilized peptide corresponding to amino acids 397–411 of  $\gamma$ -tubulin. This antibody recognizes the AFLEQF epitope corresponding to amino acids 403–408 of  $\gamma$ -tubulin. Detyrosinated tubulin (Glu-tubulin) antibody (L3) and  $\Delta$ 2-tubulin antibody (L7) were a generous gift of Dr L. Paturle-Lafanechère (25).

**Plasmon Resonance Experiments.** Quantitative analysis of peptide–tubulin interactions was performed on a BIAcore biosensor system (Pharmacia Biosensor AB, Uppsala, Sweden). The different N-biotinylated  $\gamma$ -tubulin peptides (0.5  $\mu$ g) were immobilized in PEM buffer at a flow rate of 10  $\mu$ L/min on sensor chip SA according to the manufacturer's instructions. The immobilization levels were from 600 to 1100 RU (resonance units). A nonimmobilized flow cell was used as a control. Analyte injection rate was 10  $\mu$ L/min. The surface was regenerated by injection of 10  $\mu$ L of 8 M urea. Sensorgrams were analyzed by the BIAevaluation 3.0 program (Pharmacia Biosensor AB) and kinetics constants were obtained by fitting curves to a single-site binding model.

**Binding of Biotinylated  $\gamma$ -Tubulin Peptides to in Vitro Assembled Microtubules.** Tubulin (5 mg/mL) was polymerized for 30 min at 30 °C in PEM buffer containing 5 mM

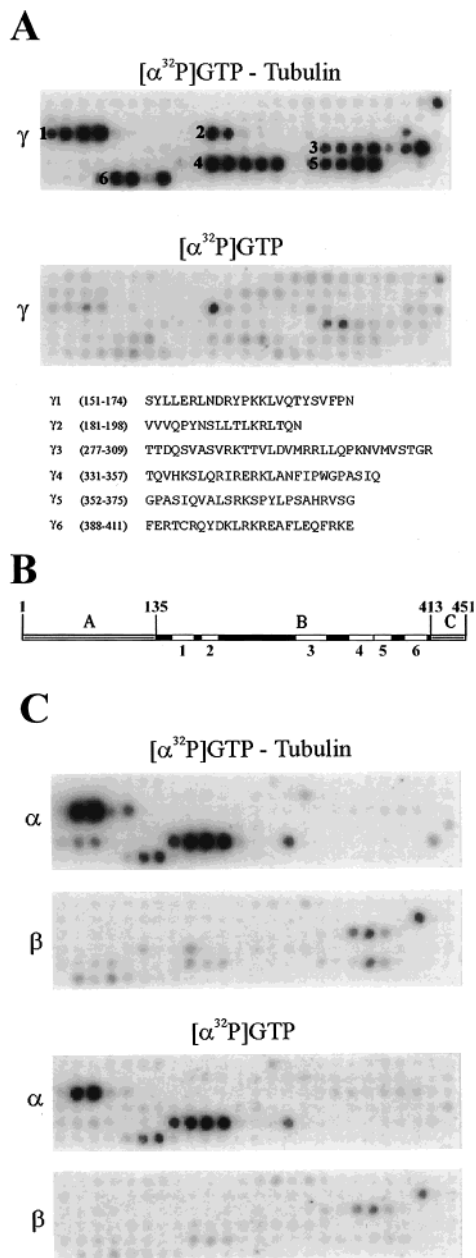


**FIGURE 1:** Tubulin binds to several peptides of  $\gamma$ -tubulin. (A) Delineation of tubulin binding sites in the  $\gamma$ -tubulin sequence, by the SPOT peptide method. A  $\gamma$ -tubulin SPOT peptide sheet was incubated with  $^{32}$ P-labeled tubulin (upper panel) or  $^{32}$ P[GTP] (lower panel) and analyzed with a PhosphorImager. The labeled peptide spots were grouped in six subsets, as indicated. Note that some spots in subsets 3 and 6 show reduced labeling. This may be due to variations in peptide synthesis efficiency or to true splitting of the tubulin binding domains. The sequences of the six corresponding tubulin binding sites are given below (numbered  $\gamma$ 1– $\gamma$ 6). (B) Diagrammatic representation of the primary amino acid sequence of  $\gamma$ -tubulin, subdomains, and the six tubulin binding sites. The primary amino acid sequence of  $\gamma$ -tubulin was subdivided on the basis of the distribution of acidic and basic amino acid residues (see Results): a basic central region (B) delineated by amino acids residues 135 and 413, an N-terminal acidic region (A), and a C-terminal acidic region (C). All of the tubulin binding sites in the  $\gamma$ -tubulin primary amino acid sequence are present in the B domain, represented by white rectangles numbered 1–6. (C) Controls: tubulin binding sites in the  $\alpha$ - and  $\beta$ -tubulin sequence.  $\alpha$ - and  $\beta$ -tubulin SPOT peptide sheets were incubated with  $^{32}$ P-labeled tubulin (upper panel) or [ $\alpha$ - $^{32}$ P]GTP (lower panel) and analyzed with a PhosphorImager. The signal observed with  $\alpha$ -tubulin sheets was apparently due to the interaction of free GTP with  $\alpha$ -tubulin peptides.

MgCl<sub>2</sub>, 20% glycerol, and 1 mM GTP. Microtubule suspension (20  $\mu$ L) was incubated with 3  $\mu$ L of N-biotinylated  $\gamma$ -tubulin peptides (1 mg/mL) for 10 min at 30 °C. Microtubules were cross-linked in 1 mL of MEM buffer (100 mM MES, pH 6.75, 1 mM EDTA, and 1 mM MgCl<sub>2</sub>) containing 50% sucrose and 1% glutaraldehyde. Cross-linked microtubules were diluted to 1/1000 in PEM buffer containing 10% glycerol at 30 °C and were sedimented onto 14 mm coverslips through a 10% glycerol cushion in PEM buffer prewarmed to 30 °C at 24000g for 15 min. Sedimented microtubules were processed for immunofluorescence as described below.

**Immunofluorescence Microscopy.** Microtubules on coverslips were fixed for 6 min in anhydrous methanol at –20 °C and subsequently washed in PBS buffer (150 mM NaCl and 10 mM sodium phosphate, pH 7.4) containing 0.1% Tween-20 in methanol and further processed for immunofluorescence. Antibodies were diluted in PBS containing 1 mg/mL BSA. L3 and L7 tubulin antibodies were diluted to 1/1000. Mouse monoclonal antibody (mAb) against biotin (Boehringer-Mannheim) was diluted to 1/1000. Goat anti-rabbit Cy2-coupled and goat anti-mouse Cy3-coupled secondary antibodies (Jackson ImmunoResearch Laboratories, West Grove, PA) were diluted to 1/1000.

Fluorescence images were digitalized by use of an RTE-CCD-1317-K/1 camera (Princeton Instruments Inc., Trenton, NJ) and IPLab Spectrum software (Signal Analytics Co., Vienna, VA).

**Structural Analysis.** For peptide mapping on tertiary structures we used the recently published tubulin structure (PDB entry 1TUB; see also ref 26). Figures were generated with Molscrip (27). Surface rendering was done with Raster 3D (28).

## RESULTS

**Characterization of Tubulin Binding Sites on Human  $\gamma$ -Tubulin.** To test the existence of tubulin binding domains on  $\gamma$ -tubulin we probed  $\gamma$ -tubulin SPOT peptide sheets with [ $\alpha$ - $^{32}$ P]GTP–tubulin complex (for details see Experimental Procedures). Such tubulin complex dissociates if tubulin is denatured (29) and this allows selective screening of peptides able to interact with native tubulin. Following incubation of  $\gamma$ -tubulin SPOT peptide sheet with [ $\alpha$ - $^{32}$ P]GTP–tubulin complex, several  $\gamma$ -tubulin peptides were labeled (Figure 1A). Signals were strong and defined six peptide domains on  $\gamma$ -tubulin. When the SPOT membrane was incubated with [ $\alpha$ - $^{32}$ P]GTP alone, only weak signals were observed and they did not significantly overlap with the [ $\alpha$ - $^{32}$ P]GTP–tubulin complex signal (Figure 1A). This result indicates that tubulin, not GTP, is responsible for the observed labeling of  $\gamma$ -tubulin domains by GTP–tubulin complex. Interestingly, the  $\gamma$ -tubulin domains were clustered in an inner part of the protein primary amino acid sequence, and this corresponded to a subdivision of  $\gamma$ -tubulin according to pI's (determined by use of DNA Star software). Amino acids 1–135 of  $\gamma$ -tubulin correspond to an acidic domain of the protein (pI = 4.28; domain A, Figure 1B). Amino acids 136–413, correspond to a basic domain (pI = 9.76; domain B, Figure 1B). Amino acids 414–451 correspond to an acidic domain of  $\gamma$ -tubulin (pI = 3.77; domain C, Figure 1B). All tubulin binding domains were located in the B domain that they almost precisely spanned (Figure 1B).



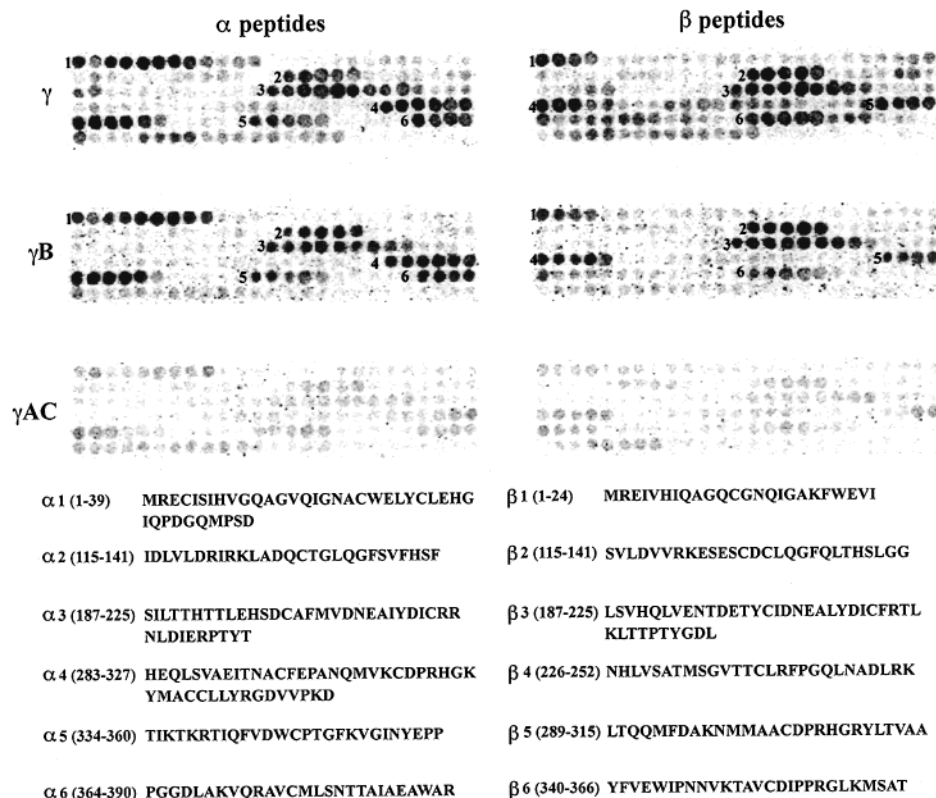
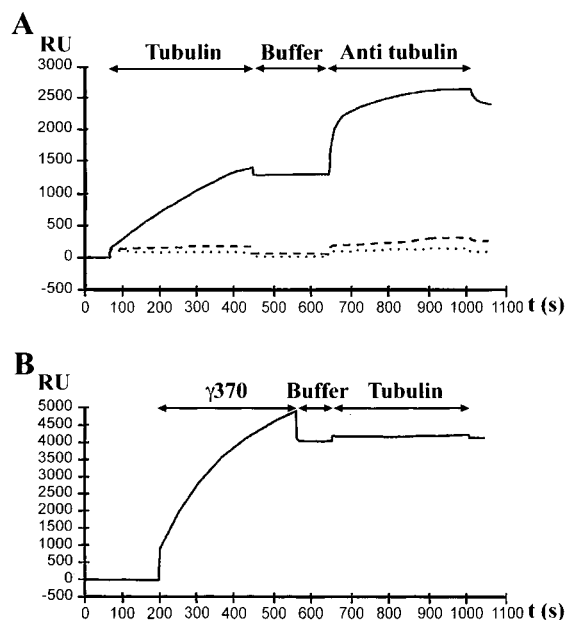


FIGURE 2: Binding of  $\gamma$ -tubulin and its domains to  $\alpha$ - and  $\beta$ -tubulin.  $\alpha$ - and  $\beta$ -tubulin peptide sheets were incubated sequentially with  $^{35}\text{S}$ -labeled full-length  $\gamma$ -tubulin and its B and AC domains and analyzed with a PhosphorImager. The peptide sequences of the six binding sites of the full-length  $\gamma$ -tubulin and the B domain of  $\gamma$ -tubulin on each  $\alpha$ - and  $\beta$ -tubulin peptide sheet are given below (numbered 1–6).

These results indicate that  $\gamma$ -tubulin contains peptides able to interact with tubulin dimers. However, before a firm conclusion could be reached, it was essential to test the specificity of the observed signals. For this, we performed a series of control experiments in which [ $\alpha$ - $^{32}\text{P}$ ]GTP–tubulin complex was incubated with SPOT membranes containing peptides of proteins other than  $\gamma$ -tubulin. These controls included incubation of  $\alpha$ - and  $\beta$ -tubulin SPOT peptide sheets with [ $\alpha$ - $^{32}\text{P}$ ]GTP–tubulin complex (Figure 1C).  $\alpha$ - and  $\beta$ -tubulins have extensive homology with  $\gamma$ -tubulin. Yet, given the extreme sensitivity of tubulin–tubulin interactions to conformational changes (induced, for instance, by GDP to GTP exchange in tubulin–nucleotide complexes), it is unlikely that such interactions rely on linear peptide sequences. Therefore, we expected to see no signal upon incubation of  $\alpha$ - and  $\beta$ -tubulin SPOT membranes with [ $\alpha$ - $^{32}\text{P}$ ]GTP–tubulin complex. Results confirmed such an expectation. Some peptide sequences were recognized on the  $\alpha$ -tubulin SPOT peptide sheet but were shown to be apparently due to the interaction of free [ $\alpha$ - $^{32}\text{P}$ ]GTP with SPOT peptides (Figure 1C). In other control experiments, tubulin complex was incubated with STOP protein sheets or with E-MAP 115 sheets. These microtubule-associated proteins comprise highly basic domains (especially STOP) and interact with tubulin in microtubules (22, 23). Yet incubations yielded negative signal (data not shown). Given the similarity of the tubulin family it could have been the case that the tubulin binding peptides in  $\gamma$ -tubulin were in fact used in intramolecular interactions involved in the folding of  $\gamma$ -tubulin rather than in interactions with tubulin heterodimers. To test this possibility we incubated  $\gamma$ -tubulin with  $\gamma$ -tubulin SPOT membranes. Results showed the

absence of  $\gamma$ -tubulin binding to peptide sequences contained within the B domain (data not shown). We conclude that the observed binding of tubulin to peptide domains of  $\gamma$ -tubulin on SPOT sheets is specific and reflects special properties of  $\gamma$ -tubulin, not observed with other tubulin binding proteins, including tubulin itself.

*Characterization of  $\gamma$ -Tubulin Binding Sites on Tubulin.* The existence of specific tubulin binding peptides on the B domain of  $\gamma$ -tubulin suggested that, reciprocally,  $\alpha$ - and/or  $\beta$ -tubulins may comprise peptides able to bind specifically to this B domain. To test this possibility,  $\alpha$ - and  $\beta$ -tubulin SPOT peptides were incubated individually with reticulocyte extracts containing in vitro translated  $^{35}\text{S}$ -labeled  $\gamma$ -tubulin or in a similar incubation containing translated B or AC domains of the protein (Figure 2). Incubation of  $\alpha$ - and  $\beta$ -tubulin SPOT sheets with in vitro translated  $\gamma$ -tubulin resulted in the labeling of six domains in both  $\alpha$ - and  $\beta$ -tubulins. An identical labeling pattern was observed when the tubulin sheets were incubated with the in vitro translated B domain of  $\gamma$ -tubulin. In contrast, the incubation of tubulin sheets with the in vitro translated AC domains of  $\gamma$ -tubulin yielded a negative signal (Figure 2). To further test the specificity of the labeling pattern observed with the B domain of  $\gamma$ -tubulin,  $\alpha$ - and  $\beta$ -tubulin sheets were incubated with in vitro translated STOP and E-MAP115. Results were completely negative (data not shown). These results indicate the existence of several specific  $\gamma$ -tubulin binding domains on both  $\alpha$ - and  $\beta$ -tubulins. We tried to identify the  $\alpha$ - and  $\beta$ -tubulin peptide(s) that interacted with each individual  $\gamma$ -tubulin peptide. For this,  $\alpha$ - and  $\beta$ -tubulin SPOT sheets were incubated with the N-biotinylated  $\gamma$ -tubulin peptides (data not shown). Results were negative, indicating that at



**FIGURE 3:** Plasmon resonance monitoring of tubulin interaction with the N-terminally biotinylated  $\gamma$ -tubulin peptides. (A) Solid line: net sensorgram (relative response in resonance units after background subtraction versus time in seconds) of tubulin injected over N-terminally biotinylated  $\gamma$ -tubulin peptide  $\gamma 5$  at a flow rate of  $10 \mu\text{L}/\text{min}$  in PEM buffer. Injection of  $225 \text{ nM}$  tubulin is indicated by a horizontal arrow, followed by injection of PEM buffer. The specificity of the binding was tested by subsequent injection of the rabbit L3 and L7 tubulin antibodies diluted  $1/100$  in PEM buffer (anti-tubulin; indicated by a horizontal arrow). Dotted line: same as above with a control sensorchip, not containing coupled peptide. Dashed line: same as above with a control sensorchip coupled to a  $\gamma$ -tubulin peptide unreactive on SPOT membranes ( $\gamma\text{UR}$ , sequence NTALNRIATDRLHIQNPS corresponds to amino acids 207–224 of the human  $\gamma$ -tubulin sequence present in the B domain). (B) Sensorgram showing injection of the  $\gamma 370$  antibody diluted  $1/100$  in PEM buffer over the same peptide  $\gamma 5$  surface as panel A, followed by tubulin injection ( $225 \text{ nM}$ ). The ability of tubulin to bind to the immobilized peptide has been inhibited by antibody binding to the immobilized peptide.

least one of the two interacting proteins must be fully folded for successful use of the SPOT peptide technique.

**Analysis of the Interaction between  $\gamma$ -Tubulin Peptides and Tubulin by Surface Plasmon Resonance.** The SPOT peptide analysis does not give information concerning the dissociation constant of protein–peptide interactions. We used plasmon resonance (in a BIAcore system) to estimate the dissociation constants of the interaction of  $\gamma$ -tubulin peptides with tubulin. N-Biotinylated  $\gamma$ -tubulin peptides corresponding to the tubulin binding domains of  $\gamma$ -tubulin were absorbed onto avidin-coated sensorchips. Injection of nanomolar tubulin solutions resulted in a significant signal (Figure 3A). The specificity of the interaction between tubulin and  $\gamma$ -tubulin peptides was tested in several ways. The identity of the molecule binding (tubulin) to the peptide surface was ascertained by the addition of tubulin antibodies (Figure 3A). Control experiments were run with either a sensorchip containing no immobilized peptide or a sensorchip containing a  $\gamma$ -tubulin peptide unreactive on SPOT sheets (peptide  $\gamma\text{UR}$ ). This unreactive peptide (NTALNRIATDRLHIQNPS) corresponds to amino acids 207–224 of the human  $\gamma$ -tubulin sequence (present in the B domain). Results showed absence of signal upon successive injection of tubulin and of tubulin antibody (Figure 3A, dotted and dashed lines). The inhibition

**Table 1:** Plasmon Resonance Measurement of  $K_d$  Values<sup>a</sup>

peptide	$K_d$ (M)
$\gamma 1$	$8.43 \times 10^{-10} \pm 5.5612 \times 10^{-10}$
$\gamma 2$	$3.14 \times 10^{-9} \pm 1.2082 \times 10^{-9}$
$\gamma 3$	$4.30 \times 10^{-10} \pm 1.6214 \times 10^{-10}$
$\gamma 4$	$1.69 \times 10^{-9} \pm 3.4522 \times 10^{-10}$
$\gamma 5$	$5.28 \times 10^{-9} \pm 3.0130 \times 10^{-9}$
$\gamma 6$	ND

<sup>a</sup> For quantitative analysis of the interaction of tubulin with sensor chip-coupled N-biotinylated  $\gamma$ -tubulin peptides, an analytical cycle has consisted in the injection of  $70 \mu\text{L}$  of tubulin at increasing concentrations ( $2, 30, 45, 57, \text{ nM}$ , and  $227 \text{ nM}$ ) in PEM buffer and a flow rate of  $10 \mu\text{L}/\text{min}$  at  $25^\circ\text{C}$ .  $K_d$  values for the interaction between N-biotinylated  $\gamma$ -tubulin peptides and tubulin were calculated with the BIAevaluation 3.0 software. Reproducible values were obtained for all  $\gamma$ -tubulin peptides except for peptide  $\gamma 6$ . ND, not determined.

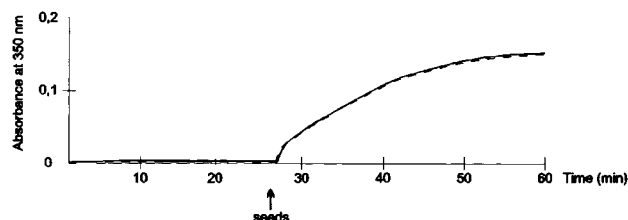


**FIGURE 4:** Spectrophotometric analysis of in vitro microtubule assembly in the presence and absence of N-terminally biotinylated  $\gamma$ -tubulin peptides. Bovine brain tubulin at  $4.5 \text{ mg}/\text{mL}$  ( $300 \mu\text{L}$ ) was assembled in spectrophotometric cells, in assembly buffer ( $80 \text{ mM}$  Pipes-KOH,  $\text{pH } 6.8$ ,  $1 \text{ mM}$  EGTA, and  $1 \text{ mM}$   $\text{MgCl}_2$ ) and  $1 \text{ mM}$  GTP at  $37^\circ\text{C}$ . No significant microtubule nucleation and assembly occurred, in the absence (solid line) or presence (dashed line) of the six N-biotinylated  $\gamma$ -tubulin peptides at equimolar concentrations with respect to tubulin. Peptides were added sequentially to the tubulin solution prior to warming. Turbidity was measured at  $350 \text{ nm}$ . At the indicated time point, a  $3 \mu\text{L}$  portion of microtubule “seeds” was added to each reaction. Seeds were formed by assembling  $50 \mu\text{M}$  tubulin in assembly buffer supplemented with  $10 \text{ mM}$   $\text{Mg}^{2+}$ ,  $5\%$  DMSO (v/v), and  $10\%$  glycerol (v/v).

of tubulin interaction with a reactive  $\gamma$ -tubulin peptide by the corresponding specific peptide antibody further demonstrated the specificity of the interaction (Figure 3B). Qualitatively similar results were observed for the six  $\gamma$ -tubulin peptides identified on SPOT sheets (data not shown). For peptide  $\gamma 6$ , estimates of the  $K_d$  fluctuated in the  $10^{-10}$ – $10^{-8}$  M range from experiment to experiment. The reason for such variations remained unclear. Precise quantitative analysis of the data was possible for the remaining five out of the six peptides (Table 1). Dissociation constants were in the nanomolar range. Thus, the peptides identified by the SPOT technique bind with high affinity to soluble tubulin.

**Effect of  $\gamma$ -Tubulin Peptides on the Assembly of Microtubules in Vitro.**  $\gamma$ -Tubulin complexes such as  $\gamma\text{TuRC}$  induce microtubule nucleation, in vitro ( $16, 30$ – $33$ ). We tested whether the binding of  $\gamma$ -tubulin peptides to tubulin dimers could affect microtubule nucleation and/or elongation during tubulin assembly in vitro. For this, pure tubulin was assembled in the presence or absence of stoichiometric amounts of  $\gamma$ -tubulin peptides. At  $1 \text{ mM}$   $\text{Mg}^{2+}$  concentration, spontaneous microtubule nucleation was minimal. Upon addition of microtubule seeds ( $20$ ), microtubule elongation occurred at the same rate regardless of the presence or absence of  $\gamma$ -tubulin peptides (Figure 4). Thus, tubulin dimers can apparently tolerate interaction with  $\gamma$ -tubulin peptides at multiple sites without showing detectable alteration of assembly behavior.

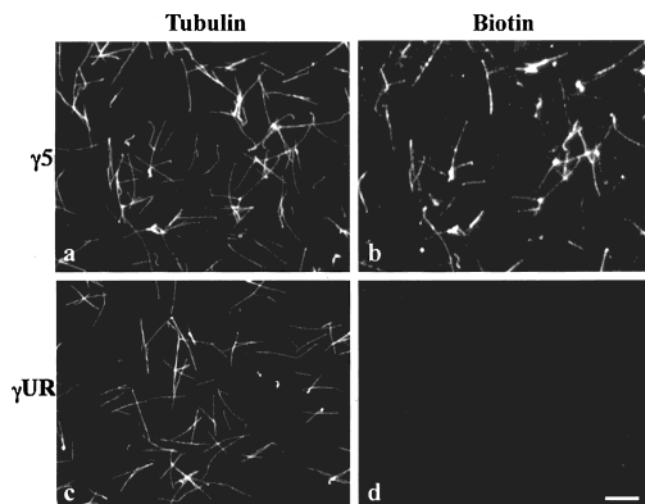


FIGURE 5: Immunofluorescence analysis of the binding of N-terminally biotinylated  $\gamma$ -tubulin peptides to in vitro assembled microtubules. Double immunostaining with tubulin L3 and L7 antibodies and a biotin antibody. Tubulin staining (a, c) and staining of bound N-terminally biotinylated  $\gamma$ -tubulin peptides  $\gamma 5$  and  $\gamma UR$  (negative control) are shown. For details, see Experimental Procedures. Bar: 5  $\mu m$ .

**Binding of  $\gamma$ -Tubulin Peptides to Microtubules.** The kinetic data shown above strongly suggest that the  $\gamma$ -tubulin peptides do not interact with domains of tubulin dimers directly engaged in tubulin–tubulin interactions. Therefore, one would expect such peptides to interact with domains of the tubulin dimers exposed on the microtubule surface. To test this possibility, we incubated microtubules with N-biotinylated  $\gamma$ -tubulin peptides and looked for microtubule decoration by these peptides following polymer centrifugation on coverslips (Figure 5). Immunofluorescence examination of the coverslips showed decoration of the spun microtubules with the tubulin binding peptides derived from  $\gamma$ -tubulin

(Figure 5b). Microtubule staining was heterogeneous: whereas a number of microtubules were fully stained, other polymers were barely visible. The origin of this heterogeneity is unclear. It was observed with all peptides, and this did not favor the possibility that it has a structural basis. Microtubule staining was completely absent when a control  $\gamma$ -tubulin peptide ( $\gamma UR$ ) was used instead of a tubulin binding peptide (Figure 5d). Thus, the tubulin-binding  $\gamma$ -tubulin peptides apparently interact with tubulin domains accessible on the surface lattice of microtubules, along the polymer length.

**Peptide Mapping on Tertiary Structures.** We have used the recently published tubulin structure (26) to map the peptides identified by SPOT analysis on tertiary protein structures. Figure 6 shows a stereoview ribbon diagram of the tubulin  $\alpha/\beta$  dimer, and Figure 7 shows a space-filling model of the dimer as it would be seen from the outside (top panel) and inside (bottom panel) of a microtubule. In these figures, the tubulin structure is viewed with  $\beta$ -tubulin at the bottom, corresponding to the plus end pointing downward for a microtubule. The peptides  $\alpha 1$ – $\alpha 6$  and  $\beta 1$ – $\beta 6$ , truncated by three amino acids at each extremity, are colored green and blue, respectively. A striking feature of Figure 7 is the large green area on the left-hand outer surface of the  $\alpha$ -subunit and the blue area running down to the lower left-hand side of the  $\beta$ -subunit. Smaller areas to the right (left in the view from the microtubule interior Figure 7B) are close to the putative lateral interprotofilament contact region. The interfaces between tubulin dimers along the protofilaments are largely unoccupied by the peptides.

On the basis of the high degree of sequence similarity to both  $\alpha$ - and  $\beta$ -tubulin, we surmise that  $\gamma$ -tubulin has a similar structure, and we have used  $\beta$ -tubulin as a tentative structural model for  $\gamma$ -tubulin. The peptides  $\gamma 1$ – $\gamma 6$  are found to cluster to surface regions on both sides of the molecule as shown in Figures 8 and 9.

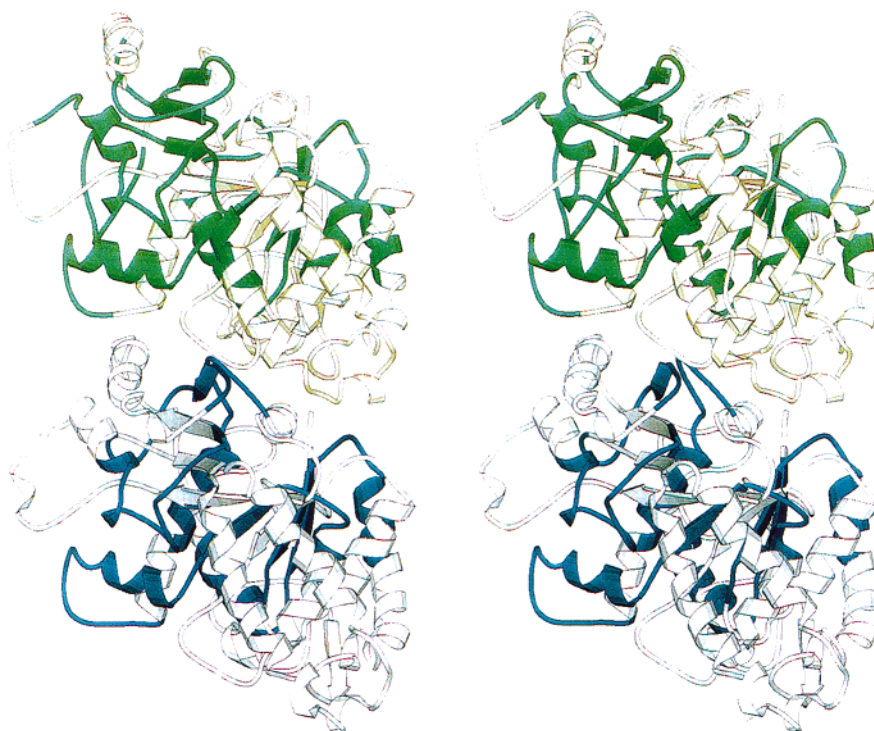


FIGURE 6: Stereoview of the tubulin dimer as viewed from a microtubule outer surface and oriented with the  $\beta$ -subunit at the bottom. Peptides  $\alpha 1$ – $\alpha 6$  are in green and peptides  $\beta 1$ – $\beta 6$  are in blue. These are peptides found to interact with  $\gamma$ -tubulin by SPOT peptide analysis.



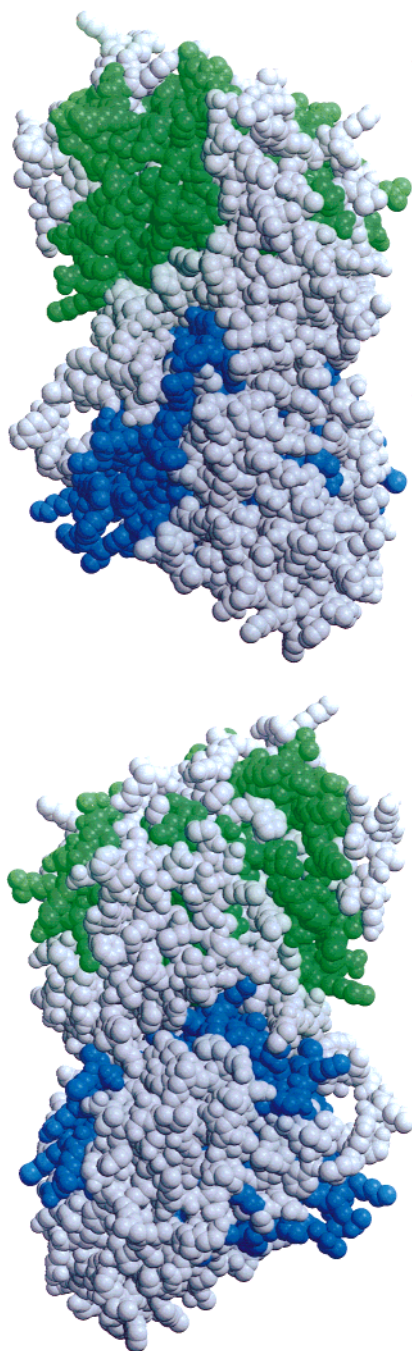


FIGURE 7: Space-filling model of the tubulin dimer. Peptides  $\alpha 1-\alpha 6$  are in green and peptides  $\beta 1-\beta 6$  are in blue. These are peptides found to interact with  $\gamma$ -tubulin by SPOT peptide analysis. The molecule is viewed (A, top) from a microtubule outer surface and oriented with the  $\beta$ -subunit at the bottom and (B, bottom) rotated by  $180^\circ$  about a vertical axis to view as from the microtubule inner surface.

These structural features show that the peptides identified by SPOT analysis are located on the surface of the three-dimensional protein structures. The surface domains correspond to tubulin domains not directly engaged in dimer-dimer interactions in microtubules. The results are fully compatible with the biochemical data presented in this article.

## DISCUSSION

This study provides direct evidence for the existence of high-affinity tubulin binding sites on  $\gamma$ -tubulin. In our search

of such sites, we have circumvented the difficulties posed by the apparent insolubility of  $\gamma$ -tubulin by using systematic mapping of tubulin binding sites on  $\gamma$ -tubulin peptides (SPOT peptide method). Such a procedure allowed assays of tubulin interaction with  $\gamma$ -tubulin domains in the absence of interference with contaminating proteins.

$\gamma$ -Tubulin has extensive sequence homology with tubulin (34). This observation has suggested that the two proteins may have related biochemical properties including the capability to associate in homo- or heterocomplexes. Our data confirm this prediction but also suggest that the biochemical mechanisms involved in the interaction of  $\gamma$ -tubulin with tubulin differ significantly from those involved in tubulin self-assembly. The binding of native tubulin dimers to  $\gamma$ -tubulin apparently occurs through several high-affinity linear binding sites. This type of association is compatible with the need to form stable cooperative complexes between the two proteins. In contrast, the same binding mechanism would be hardly compatible with the highly dynamic protein-protein association observed in the case of tubulin assemblies. Hence, the absence of peptide with high affinity for native tubulin dimers in both  $\alpha$ - and  $\beta$ -tubulin seems logical. We found it remarkable that  $\gamma$ -tubulin and tubulin contained homologous peptides with completely different tubulin binding capability.

Using *in vitro* translated  $\gamma$ -tubulin as a probe, we also find specific binding of  $\gamma$ -tubulin to  $\alpha$ - and  $\beta$ -tubulin peptides on SPOT membranes. These findings have to be interpreted with some caution. The cell extracts used for  $\gamma$ -tubulin translation contain many proteins in addition to  $\gamma$ -tubulin and some of these proteins may mediate indirect interaction between  $\gamma$ -tubulin and tubulin peptides. However, only  $\gamma$ -tubulin, not other proteins translated in similar cell extracts, yielded positive signals on  $\alpha$ - and  $\beta$ -tubulin SPOT membranes and the specificity of the detected interaction was further demonstrated by the unique reactivity of the B subdomain of  $\gamma$ -tubulin.

We find that  $\gamma$ -tubulin peptides bind with nanomolar  $K_d$  on tubulin. These data agree with previous estimations made with *in vitro* transcribed  $\gamma$ -tubulin preparations (35). Such a high affinity of  $\gamma$ -tubulin for tubulin poses intriguing questions concerning the mechanism and regulation of microtubule nucleation. When centrosomes are incubated with soluble tubulin, the number of microtubules nucleated per centrosome increases in response to variations of the free tubulin concentration in the  $10^{-5}$  M range (20). This may suggest that centrosomal nucleation complexes are not saturated with tubulin at lower concentrations. However, with a nanomolar  $K_d$  for the  $\gamma$ -tubulin-tubulin binding reaction, nucleation complexes on centrosomes should be saturated at about  $10^{-8}$  M free tubulin concentration. What could be the explanation for such a marked discrepancy? One possibility is that the microtubule number is controlled by dynamic instability, independently of the number of centrosomal nucleation sites (36). Other explanations are possible. For instance, microtubule nucleation on centrosomes may be controlled by kinetic factors, the limiting parameter being the on rate of the tubulin association with the nucleation sites.

We find that the  $\gamma$ -tubulin peptides bind along the length of assembled microtubules and do not measurably interfere with tubulin polymerization. These data suggest that the

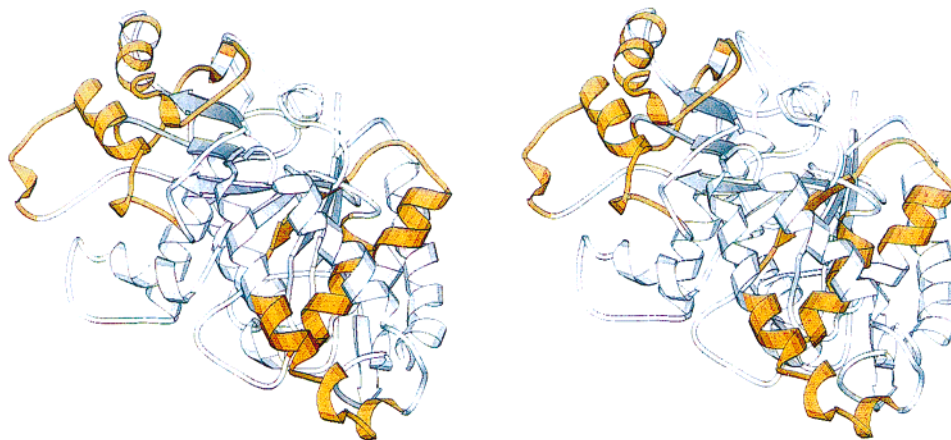


FIGURE 8: Stereoview of the putative  $\gamma$ -tubulin structure using  $\beta$ -tubulin as a tentative structural model for  $\gamma$ -tubulin. The model molecule corresponds to a  $\beta$ -tubulin molecule viewed from a microtubule outer surface with the  $\beta$ -subunit at the bottom. The peptides found to interact with  $\alpha$ - and  $\beta$ -tubulin are in yellow.

peptides do not bind to tubulin domains involved in either lateral or longitudinal tubulin–tubulin interaction. The data also suggest that  $\gamma$ -tubulin itself may bind to the side of assembled microtubules, at least in some circumstances.  $\gamma$ -Tubulin has been found to be a microtubule minus-end-binding molecule (18, 35), but the presence of  $\gamma$ -tubulin along the sides of microtubule in spindles has been reported (37).

We have used the recently published tubulin structure (26) to map the peptides identified by SPOT analysis. Peptides were located on the surface of the three-dimensional structures of  $\alpha$ -,  $\beta$ -, and  $\gamma$ -tubulin and clustered to lateral regions of the proteins. None of the tubulin peptides found to interact with  $\gamma$ -tubulin was located in domains involved in dimer–dimer interactions in microtubules. Therefore, the structural analysis was fully compatible with the biochemical data.

How do the data relate to microtubule nucleation by  $\gamma$ -tubulin? There are currently two models of  $\gamma$ -tubulin-induced microtubule nucleation (16, 38). In one (16),  $\gamma$ -tubulin rings or spirals provide a direct template for the formation of a cylindrical microtubule via the end-to-end attachment of tubulin dimers, giving lengthwise growth along the protofilaments perpendicular to the plane of the ring. In the other (38), a short  $\gamma$ -tubulin protofilament projection acts as a template to nucleate a tubulin sheet by a sideways interaction like that between protofilaments. The sheet grows sideways, folding into a cylinder, and lengthwise by protofilament elongation. Looking at the  $\alpha\beta$  dimer tubulin as it would be seen from the outside of the microtubule, and at the  $\gamma$ -tubulin model in the same orientation, shows the putative interaction patches to be mainly toward the sides of all the subunits. Our data tend to argue in favor of the second model of microtubule nucleation (38). However, the  $\gamma$ -tubulin ring model (16) does involve a lateral interaction between one  $\gamma$ -tubulin molecule and a tubulin dimer, and the  $\gamma$ -tubulin protofilament model (38) involves a longitudinal interaction between the terminal  $\gamma$ -tubulin molecule and the adjacent  $\alpha$ -subunit. Therefore the two models differ chiefly in the relative importance of the two interactions. Furthermore, SPOT analysis identifies binding sites that do not require the correct folding of both protein partners. It may be that additional binding sites that require the correct

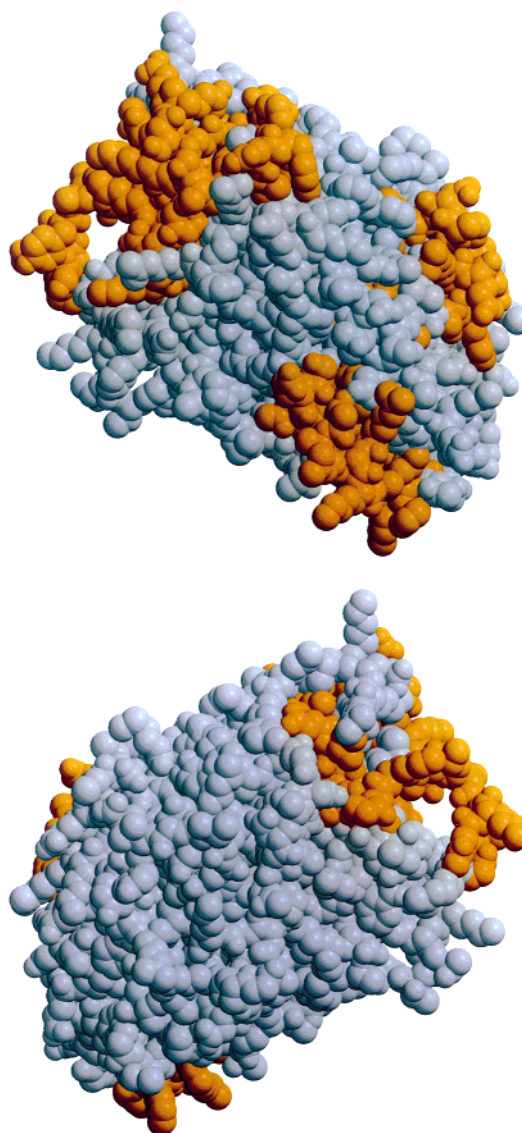


FIGURE 9: Space-filling model of  $\gamma$ -tubulin structure using  $\beta$ -tubulin as a tentative structural model for  $\gamma$ -tubulin. The peptides found to interact with  $\alpha$ - and  $\beta$ -tubulin are in yellow. The model molecule corresponds to (A, top) a  $\beta$ -tubulin molecule viewed from a microtubule outer surface with the  $\beta$ -subunit at the bottom and (B, bottom) rotated by  $180^\circ$  about a vertical axis to view as from the microtubule inner surface.



folding of both protein partners have escaped detection in the present study.

The SPOT analysis done in this study provides a map of the tubulin binding domains of  $\gamma$ -tubulin. We believe that the same strategy may be useful for the mapping of the  $\gamma$ -tubulin domains involved in the interaction of the protein with other partners. The search for new  $\gamma$ -tubulin partners may also be facilitated by the sorting of the  $\gamma$ -tubulin domains involved or not in high-affinity interactions with tubulin dimers.

## ACKNOWLEDGMENT

We thank Dr. E. Mandelkow, Dr. S. Pistor, Dr. M. Block, and Dr. C. Bosc for useful advice during this work; Dr. A. Tiepold, Dr. B. Kornak, and Dr. J. Garin for help in peptide synthesis; and Mrs N. Collomb for expert technical assistance.

## REFERENCES

- Cande, W. (1990) *Curr. Opin. Cell Biol.* 2, 301–305.
- Huang, B. (1990) *Curr. Opin. Cell Biol.* 2, 28–32.
- Raff, J. W., Kellog, D. R., and Alberts, B. M. (1993) *J. Cell Biol.* 121, 823–835.
- Geissler, S., Pereira, G., Spang, A., Knop, M., Souès, S., Kilmartin, J., and Schiebel, E. (1996) *EMBO J.* 15, 3899–3911.
- Détraves, C., Mazarguil, H., Lajoie-Mazenc, I., Julian, M., Raynaud-Messina, B., and Wright, M. (1997) *Cell Motil. Cytoskeleton* 36, 179–189.
- Knop, M., and Schiebel, E. (1997) *EMBO J.* 16, 6985–6995.
- Tassin, A. M., Celati, C., Paintrand, M., and Bornens, M. (1997) *J. Cell Sci.* 110, 2533–2545.
- Dictenberg, J. B., Zimmerman, W., Sparks, C. A., Young, A., Vidair, C., Zheng, Y., Carrington, W., Fay, F. S., and Doxsey, S. J. (1998) *J. Cell Biol.* 141, 163–174.
- Moritz, M., Zhen, Y., Alberts, B. M., and Oegema, K. (1998) *J. Cell Biol.* 142, 775–786.
- Tassin, A. M., Celati, C., Moudjou, M., and Bornens, M. (1998) *J. Cell Biol.* 141, 689–701.
- Oakley, C. E., and Oakley, B. R. (1989) *Nature* 338, 662–664.
- Joshi, H. C. (1994) *Curr. Opin. Cell Biol.* 6, 55–62.
- Pereira, G., and Schiebel, E. (1997) *J. Cell Sci.* 110, 295–300.
- Martin, M. A., Osmani, S. A., and Oakley, B. R. (1997) *J. Cell Sci.* 110, 623–633.
- Stearns, T., Evans, L., and Kirschner, M. (1991) *Cell* 65, 825–836.
- Zheng, Y., Wong, M. L., Alberts, B. M., and Mitchison, T. (1995) *Nature* 378, 578–583.
- Vassilev, A., Kimble, M., Silflow, C. D., LaVoie, M., and Kuriyama, R. (1995) *J. Cell Sci.* 108, 1083–1092.
- Melki, R., Vainberg, I. E., Chow, R. L., and Cowan, N. J. (1993) *J. Cell Biol.* 122, 1301–1310.
- Frank, R. (1992) *Tetrahedron* 48, 9217–9232.
- Mitchison, T., and Kirschner, M. (1984) *Nature* 312, 232–242.
- Zheng, Y., Jung, M. K., and Oakley, B. R. (1991) *Cell* 65, 817–823.
- Bosc, C., Cronk, J. D., Pirollet, F., Watterson, M. D., Haiech, J., Job, D., and Margolis, R. L. (1996) *Proc. Natl. Acad. Sci. U.S.A.* 93, 2125–2130.
- Masson, D., and Kreis, T. E. (1993) *J. Cell Biol.* 123, 357–371.
- Niebuhr, K., and Wehland, J. (1997) *Immunology Methods Manual*, pp 797–800.
- Paturle-Lafanechère, L., Manier, M., Trigault, N., Pirollet, F., Mazarguil, H., and Job, D. (1994) *J. Cell Sci.* 107, 1529–1543.
- Nogales, E., Wolf, S. G., and Downing, K. H. (1998) *Nature* 391, 199–203.
- Kraulis, P. J. (1991) *J. Appl. Crystallogr.* 24, 946–950.
- Merritt and Bacon (1997) *Methods Enzymol.* 277, 505–524.
- Job, D., Pabion, M., and Margolis, R. L. (1985) *J. Cell Biol.* 101, 1680–1689.
- Vogel, J. M., Stearns, T., Rieder, C. L., and Palazzo, R. E. (1997) *J. Cell Biol.* 137, 193–202.
- Moritz, M., Braunfeld, M. B., Fung, J. C., Sedat, J. W., Alberts, B. M., and Agards, D. A. (1995) *J. Cell Biol.* 130, 1149–1159.
- Moritz, M., Braunfeld, M. B., Sedat, J. W., Alberts, B. M., and Agards, D. A. (1995) *Nature* 378, 638–640.
- Oakley, B. R. (1995) *Nature* 378, 555–556.
- Burns, R. G. (1995) *J. Cell Sci.* 108, 2123–2130.
- Li, Q. and Joshi, H. C. (1995) *J. Cell Biol.* 131, 207–214.
- Dogterom, M., Maggs, A. C., and Leibler, S. (1995) *Proc. Natl. Acad. Sci. U.S.A.* 92, 6683–6688.
- Lajoie-Mazenc, I., Tollon, Y., Détraves, C., Julian, M., Moisan, A., Gueth-Hallonet, C., Debec, A., Salles-Passador, I., Pujet, A., Mazarguil, H., Raynaud-Messina, B., and Wright, M. (1994) *J. Cell Sci.* 107, 2825–2837.
- Erickson, H. P., and Stoffler, D. (1996) *J. Cell Biol.* 135, 5–8.

BI990895W